

Article

Not peer-reviewed version

---

# Integrating Geosynthetics and Vegetation for Erosion Control Applications

---

[Tatiana Olinic](#)\*, [Ernest-Daniel Olinic](#)\*, [Ana-Cornelia Butcaru](#)

Posted Date: 29 October 2024

doi: 10.20944/preprints202410.2332.v1

Keywords: roots reinforcement; shear strength parameters; erosion control; geosynthetics



Preprints.org is a free multidisciplinary platform providing preprint service that is dedicated to making early versions of research outputs permanently available and citable. Preprints posted at Preprints.org appear in Web of Science, Crossref, Google Scholar, Scilit, Europe PMC.

Copyright: This open access article is published under a Creative Commons CC BY 4.0 license, which permit the free download, distribution, and reuse, provided that the author and preprint are cited in any reuse.

## Article

# Integrating Geosynthetics and Vegetation for Erosion Control Applications

Tatiana Olinic <sup>1,\*</sup>, Ernest-Daniel Olinic <sup>2</sup> and Ana-Cornelia Butcariu <sup>3</sup>

<sup>1</sup> Faculty of Land Reclamation and Environmental Engineering, University of Agronomic Sciences and Veterinary Medicine Bucharest, Romania

<sup>2</sup> Faculty of Hydrotechnics, Technical University of Civil Engineering Bucharest

<sup>3</sup> Research Center for Studies of Food Quality and Agricultural Products, USAMV Bucharest

\* Correspondence: tatiana.olinic@fifim.ro

**Abstract:** The stability of slopes is a critical challenge in various civil engineering projects, such as embankments, cut-slopes, landfills, dams, transportation infrastructure, and riverbank restoration. Stabilizing slopes using bioengineering methods is a sustainable approach that limits the negative impact of engineering works; such methods should be implemented and adopted worldwide. Geosynthetic materials and plant roots are sustainable for preventing erosion and surface landslides. The plants used for this paper are known to have beneficial effects on erosion control, namely *Festuca arundinaceus*, *Dactylis glomerata*, *Phleum pratensis*, *Trifolium pratense*, and *Trifolium repens*. Using vegetation as a bio-reinforcement method is often more cost-effective and environmentally friendly than traditional engineering solutions. The paper interprets the erosion process that occurred on sandy slopes protected by organic soil layers and geosynthetic materials under rainfall simulation on scale model tests.

**Keywords:** roots reinforcement; shear strength parameters; erosion control; geosynthetics

## 1. Introduction

The stability of slopes is a critical challenge in various civil engineering projects, such as embankments [1], cut-slopes, landfills [2], dams, transportation infrastructure [3], and riverbank restoration [1,4]. Geosynthetic materials for erosion control have demonstrated their effectiveness in improving shallow slope stability. These materials can reinforce the topsoil, increasing its shear strength and reducing the risk of shallow slope failures. Alongside the use of geosynthetics for erosion control, the use of vegetation in slope stabilization systems has gained increasing attention. Through their extensive root systems, living plants can stabilize shallow slopes [5] and offer sustainable, long-term solutions. Researchers have explored the synergistic relationship between geosynthetics and living plants, recognizing the potential to create a comprehensive and sustainable approach to slope stabilization.

Ecological slope protection not only has the function of traditional slope protection; it also integrates various aspects such as landscape, culture, and ecology, thereby achieving the maintenance and restoration of natural ecosystems [6]. The roots of plants developed on the entire slope generate both hydrological and mechanical effects, contributing to erosion protection and slope stabilization of the complex as a whole [7]. Also, it is considered that this practice is strongly dominated by empiricism [4].

Tension-bearing plant roots infiltrate soil pores, enhancing the shear strength of the soil-root matrix. In past decades, mechanical root reinforcement has been extensively quantified experimentally and analytically, and this effect is usually included in slope stability calculations [8].

In civil and environmental engineering projects, geosynthetic materials for erosion control are often essential during construction to mitigate soil loss and prevent sediment runoff in the short and long term

to support the growth and maintenance of dense vegetation. This vegetation, after a period, protects slopes from splash and sheet erosion, thereby effectively preventing the formation of rill erosion [9].

Water-induced erosion degrades soil quality, leading to reduced crop yields. Understanding how crop yields respond to soil erosion is crucial for evaluating agriculture's susceptibility to such degradation. Research conducted by [10] suggests that quantifying the reduction in crop yields due to erosion is a challenging topic. Soil erosion occurs when topsoil is displaced by natural forces such as wind and water [11]. The erosion process increases with greater soil exposure, especially during rain or windstorms. When topsoil is lost, the soil's most nutrient-dense layer is removed, leading to a decline in overall soil quality.

Additionally, many studies investigate how soil erosion affects soil and plant properties, as well as its impact on associated ecosystem services. Research conducted by [12] emphasized that soil erosion has profound consequences on the functioning of ecosystems and the services they provide. They recommended soil conservation and ecosystem restoration measures to prevent further degradation and to protect soil, biodiversity, and agricultural productivity. Turcu et al. (2024) point out that plowing in hilly areas can affect soil surface roughness, altering flow rate, water infiltration time, and infiltration and runoff processes [13].

Vegetation affects slope stability and erosion through mechanical and hydrological effects. Yen, cited by Cazzuffi et al., 2014, classified the root structure into five classes based on branching patterns: VH-type, H-type, V-type, R-type, and M-type. The branching pattern scheme was recreated based on Yen's original work and cited by [14] in Figure 1. Based on the analysis performed by Yen, he reported that the best roots used for slope stabilization and wind resistance are the H-type and the VH-type patterns.

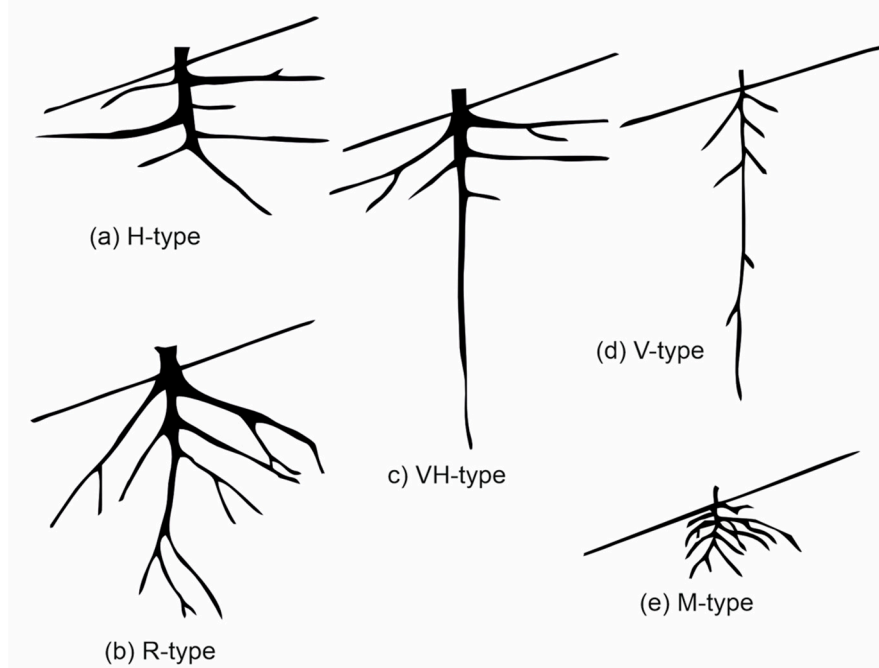


**Figure 1.** The root structure classified by Yen (recreated figure).

A study by Mairaing et al., 2024, investigated the significance of root systems of various plant species well known for erosion control benefits and slope stabilization in the highland areas of Thailand. The plants chosen for the research were either native to or well-adapted to Thailand's mountainous regions, recognized for their effectiveness in preventing erosion. These roots provided a strong anchor within the soil, particularly on steep terrains. Additionally, extensive lateral roots contributed to the distribution of forces on the soil surface, which helped prevent surface erosion from water runoff. The study ultimately recommended using plants with robust root systems for rehabilitation and slope stabilization efforts in mountainous areas [15].

Engineering judgment involves using various methods, including horizontal drains, slope reinforcement techniques, soil hardening measures, surface water management techniques,

groundwater control methods, and proper vegetation management [16], to prevent slope failure under rainfall conditions.

Stabilizing slopes using bioengineering methods is a sustainable approach that limits the negative impact of engineering works; such methods should be implemented and adopted worldwide.

## 2. Materials and Methods

### 2.1. Used Materials

#### 2.1.1. Geosynthetics for Erosion Control—Geomats

From a design perspective, using geosynthetics in engineering applications now represents a sustainable and well-established technological solution. Geosynthetics, durable construction materials used in engineering, exemplify a successful approach to sustainable development [17].

Geomats- three-dimensional geosynthetic materials- are widely used to prevent soil erosion caused by wind or water. These porous structures are placed on slope surfaces and are particularly effective on steep slopes, providing stability for plant roots, encouraging vegetation growth, and strengthening erosion resistance [18,19]. These erosion control systems may be required in civil and environmental engineering projects as a short-term solution during construction to limit soil loss and sediment runoff from the site and as a long-term solution to establish dense vegetation coverage that protects slopes from splash and sheet erosion while preventing rill erosion [9].

Geosynthetics provide an affordable, long-lasting, and eco-friendly approach to soil erosion control and slope stabilization in diverse civil engineering projects [20]. Their capacity to blend with natural environments and their mechanical solid properties render them essential in contemporary erosion control methods.

The geosynthetic materials used for erosion control in this study consisted of two HDPE (High-Density Polyethylene) and PP (Polypropylene) geomatics (named GEC1 and GEC2) and one geobanket made from biodegradable materials (Jute, named GEC3) (Figure 2). These materials were provided strictly for this study by two manufacturing and supplying companies with geosynthetic materials.

GEC1 is a PP-based, three-dimensional synthetic erosion control solution designed to permanently reinforce the grass-root matrix, providing long-term surface erosion protection. This product is ideal for applications where vegetation needs continuous support to shield the soil from weather and water erosion. Its densely interwoven strands mimic the function of a root system, binding soil particles and bonding fertile humus to strengthen the soil structure. The mechanical properties are tensile strength in the length direction of 1.3 kN/m and in the cross direction of 0.5 kN/m; the strain at maximum strength in both directions is 50% ( $\pm 25\%$ ). The physical properties are melting point of 150°C, mass per unit area of 350 g/m<sup>2</sup> ( $\pm 40$ ), PP single filament diameter of 500  $\mu\text{m}$  ( $\pm 30\%$ ), void index above 90%, and thickness at 2 kPa of 18 mm ( $\pm 2$  mm).

GEC2 comprises three layers: a rhombic HDPE net as the base layer, a bi-oriented PP reinforcement layer in the middle, and another HDPE net that gives the product its wave-like shape and thickness. This material is designed to support vegetation growth and provide erosion control on slopes and channels, utilizing its volumetric structure. The wave-shaped design helps trap newly laid soil and seeds. The mechanical properties provided is the tensile strength of 3.5 kN/m at 20% elongation. The physical properties are a mass per unit area of 340 g/m<sup>2</sup> ( $\pm 40$ ) and a 20 to 25 mm thickness.

The GEC3 jute fiber fabric is designed for temporary use, effectively reducing soil erosion from heavy rainfall, supporting initial vegetation growth, and serving as interception storage. Made from renewable and biodegradable jute fibers, the product consists of double-twisted jute woven in the warp (longitudinal) and weft (transverse) directions using a plain weave. Its variable and flexible mesh structure is ideal for promoting plant growth. The number of threads shading percentage of approx. 50 %, and thread thickness of approx. 2.65 mm provides a balance between erosion protection



and greening potential. With its high water absorption capacity, the fabric minimizes erosion while acting as a moisture reservoir, gradually releasing water from the jute fibers. This material has a tensile strength of 5 to 7.5 kN/m and a mesh spacing from wrap-to-wrap x weft-to-weft of 20 x 30 mm.

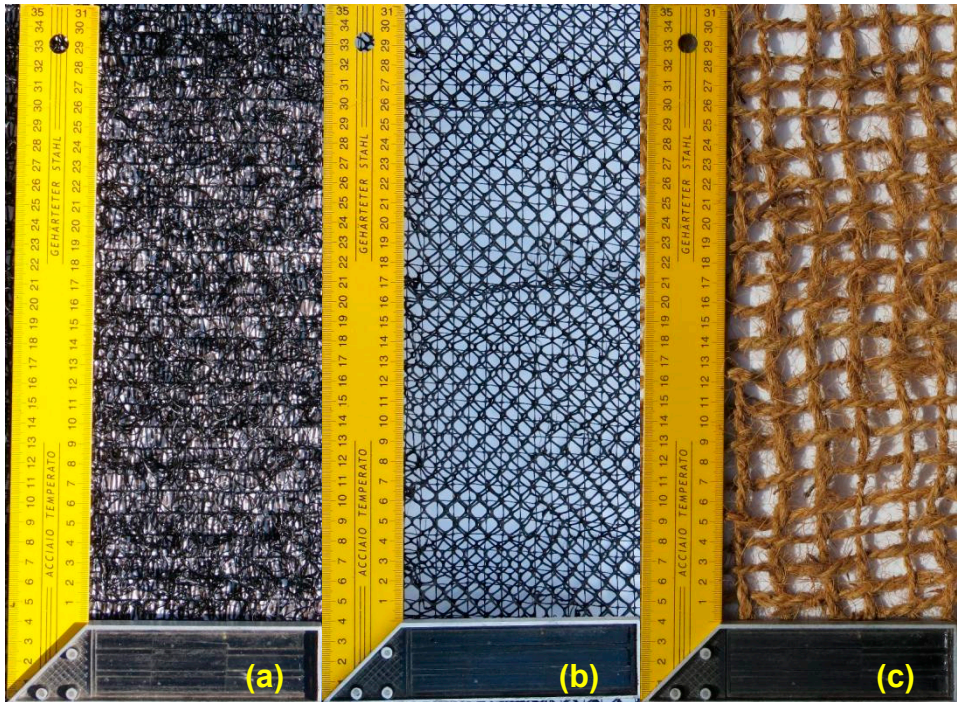


Figure 2. The geosynthetic materials used for this study: (a) GEC 1, (b) GEC 2, and (c) GEC 3.

2.1.2. Properties of Used Soils

The organic soil (OS) used in this study is a natural product commonly used for gardening, with an organic matter content ranging between 60-80% and a pH value of 5 to 7. Geotechnical characteristics of the OS are internal friction angle of 19.57° and cohesion of 36.11 kPa. The soil used in all the tests is known as very erodible soil - sandy soil. From the granulometric perspective, medium to coarse sand with poor gradation, according to SR EN ISO 14688:2-2018 [21] (Figure 3). Geotechnical characteristics of the bare sand (BS) are a specific gravity of 2.65 g/cm<sup>3</sup>, internal friction angle of 32.94°, and cohesion of 1.24 kPa.

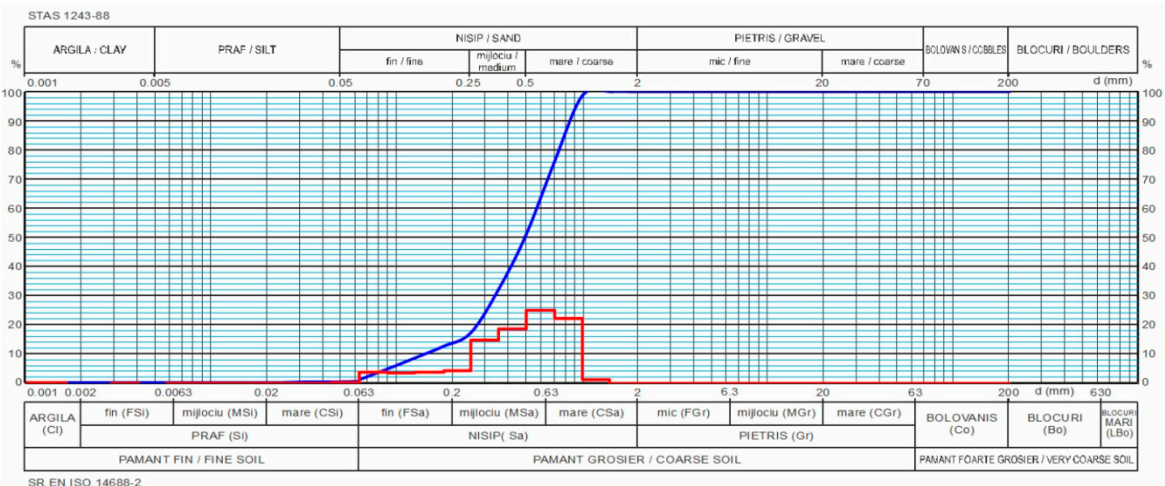


Figure 3. Grain size distribution of the sand sample.

2.1.3. Vegetation

The plants used for this paper are known to have beneficial effects in erosion control, namely *Festuca arundinaceous*, *Dactylis glomerata*, *Phleum pratensis*, *Trifolium pratense*, and *Trifolium repens*. Two seed mixtures were studied for the stage aimed at determining the optimal thickness of the topsoil layer for plant roots: Mix 1 and Mix 2. The plant mixture used in Mix 1 is recommended for use on artificial slopes according to the Design Guide GE 027-1997. This mixture has the following composition: *Dactylis glomerata* 40%, *Festuca arundinaceous* 30%, and *Trifolium pratense* 30%. The Mix 2 is commonly used in grassland areas in Romania, specifically: *Festuca arundinaceous* 25%, *Dactylis glomerata* 25%, *Phleum pratensis* 20%, *Trifolium pratense* 10%, and *Trifolium repens* 20%. The seeds used in the research were sourced from a forestry research center, and all the seeds are well-known for being used for grassland.

Herbaceous plants have extensive fibrous root systems that create a network within the soil, binding soil particles together. The roots of herbaceous plants act as natural reinforcements, enhancing the mechanical properties of the soil. This is especially important in shallow soil layers, where herbaceous roots most effectively stabilize the surface. The roots also absorb significant amounts of water from the soil, reducing soil moisture content. These plants are generally fast-growing, which allows them to establish a protective cover on slopes quickly. Their ability to adapt to different environmental conditions makes them a flexible choice for slope stabilization projects [22].

The research conducted by Lv et al. in 2024 indicated that the roots of herbaceous plants significantly impact the biological reinforcement of slopes, particularly due to their ability to strengthen soil structure. Additionally, the researchers found that the density and depth of the root system are essential factors in improving soil stability. Plants with deeper and denser roots provided greater protection against shallow landslides than those with smaller roots [23].

2.2. Testing Methodology

To observe and quantify the beneficial effect of plant roots and geosynthetic materials on the stability and geometry of slopes, the following parameters were determined: the optimal thickness of the soil layer for root development, the characteristics and shape of the roots, shear strength parameters on control samples and root samples taken from various depths, the design of a scaled experimental model to observe the erosion phenomenon, as well as the design and calibration of a torrential rainfall simulator.

2.2.1. Optimum Organic Soil Thickness

To determine the optimal thickness of the OS layer for proper root development, seeds were sown in cylindrical containers filled with different amounts of sand and OS. The cylindrical containers, with a height of 27 cm and a diameter of 8 cm, were filled with layers of 5, 10, 15, and 20 cm of sand and 0, 5, 10, 15, and 20 cm of organic soil (Figure 4). Seeds from Mix 1 and Mix 2 were sown (on 30.09.2022) in single amounts (40 g/m<sup>2</sup>) and double amounts (80 g/m<sup>2</sup>), resulting in a total of 20 containers. The containers were placed in the University of Agronomic Sciences and Veterinary Medicine greenhouse in Bucharest at a constant temperature of 24°C and a controlled light and humidity throughout the autumn and winter.

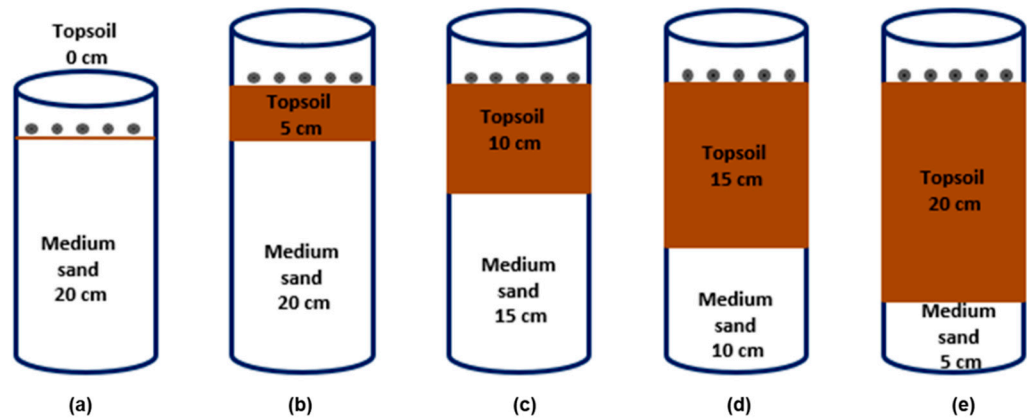


**Figure 4.** The distribution of the topsoil layer in the cylindrical containers to determine the optimum OS thickness: (a) 0 cm OS, (b) 5 cm OS, (c) 10 cm OS, (d) 15 cm OS, and (e) 20 cm OS.

For this activity, visual observations were made regarding plant germination, stem and leaf development, and root growth.

### 2.2.2. Scanning of Roots with WinRHIZO

The WinRHIZO system was used to assess root development in different variants. Leguminous and Gramineae plants were used in a mixed composition of *Festuca arundinacea* (25%), *Dactylis glomerata* (25%), *Phleum pratense* (20%), *Trifolium pratense* (10%), and *Trifolium repens* (20%), grown in OS layers with thicknesses of 0, 5, 10, and 20 cm.

WinRHIZO, created by Regent Instruments Canada Inc., includes an Epson 11000XL scanner and software for image processing [24]. It is a high-performance system that allows morphological measurements of the root system and analyzes a series of essential parameters, including root system length (cm), root system projection (cm<sup>2</sup>), root surface area (cm<sup>2</sup>), root volume (cm<sup>3</sup>), average root diameter (mm), root classes according to scanned diameter, and roots apical tips. Additionally, it eliminates a series of possible errors in analysis, such as individually calculating overlaps and removing foreign bodies that may remain after root cleaning (Figure 5).

The roots of each sample were washed with tap water to remove soil. They were then manually measured for length using a linear meter, placed into a 100 ml plastic tube, and submerged in water for volume measurement.

The roots of each sample were then scanned using WinRHIZO root-scanning equipment and software, allowing root length and volume to be measured from the scanned images. In the present study, we compared the size and root volume measured by the software with those determined manually.

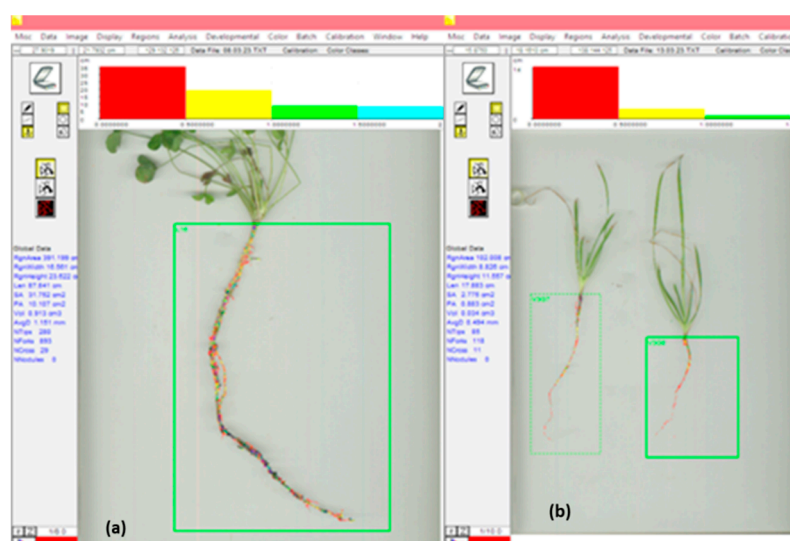


**Figure 5.** Scanning images analyzed with WinRHIZO software: (a) Leguminous plant, (b) Gramineae plants.

### 2.2.3. Shear Test Strength

The direct shear test was carried out using the Shearmatic automatic direct/residual shear machine with programmable pneumatic loading produced by Wykeham Farrance. According to the geotechnical test method standard SR EN ISO 17892-10:2019 [24], the shear strength parameters were determined in unconsolidated – undrained saturated conditions (UU<sub>sat</sub>) performed on initially saturated samples, with a shearing speed of 1.00 mm/min (Figure 6). The UU<sub>sat</sub> tests of the root-soil complex were conducted under various effective confining pressures (25 kPa, 50 kPa, and 75 kPa) after a growth period of 150 days.



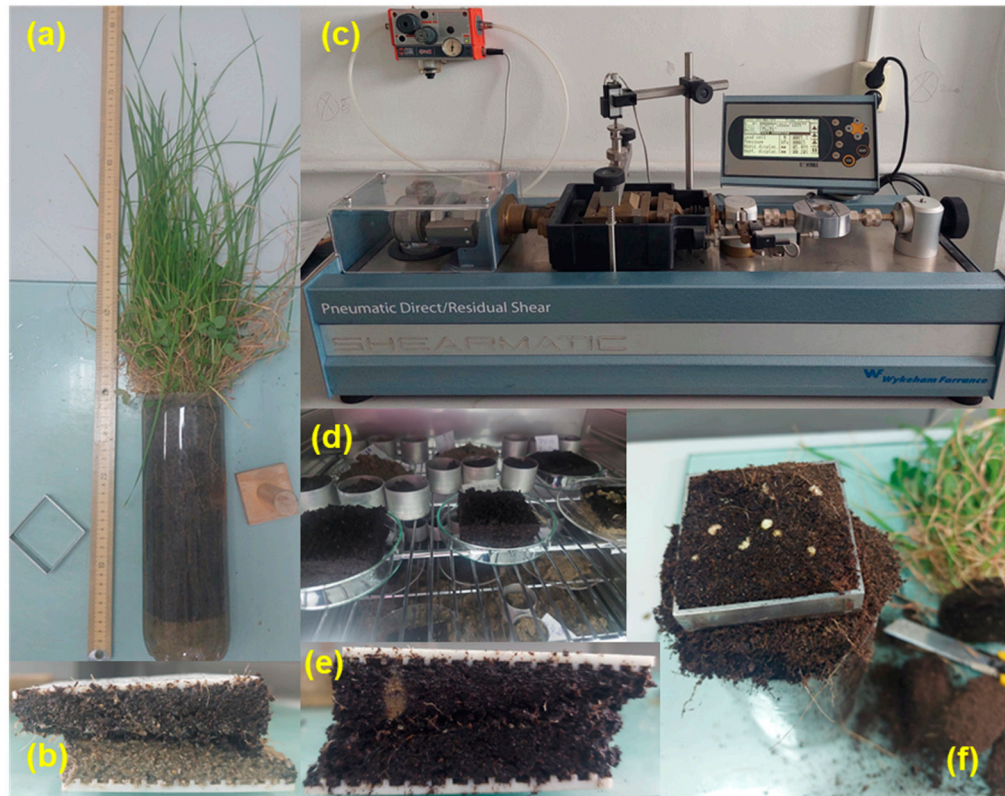


**Figure 6.** The direct shear methodology: (a) the sample of 20 cm OS with living vegetation, (b) sheared sample at the interface between OS and sand with roots, (c) the Shearmatic automatic direct/residual shear machine, (d) sheared samples in the oven, (e) OS with roots sheared sample, and (f) sample taken from the upper part of the cylinder.

The Mohr-Coulomb failure criterion suggests that material failure occurs due to the combined effects of normal stress ( $\sigma_n$ ) and shear stress ( $\tau$ ). In the context of a soil-root composite, the presence of roots can influence the overall shear strength of the soil, effectively increasing its resistance to failure. The criterion is represented mathematically by the Mohr-Coulomb equation:

$$\tau_f = c' + (\sigma_n - u) * \tan\phi' + c_r, (kPa) \quad (1)$$

where  $\tau_f$  is the shear strength (kPa),  $c'$  is the cohesion force,  $\sigma_n$  is the vertical stress (kPa),  $u$  is the total pore water pressure (kPa),  $\phi'$  is the internal friction angle ( $^\circ$ ), and  $c_r$  is the cohesion force added by roots (kPa), often termed root-induced cohesion or pseudo-cohesion.

The term  $(\sigma_n - u)$  represents the effective normal stress, which is the actual stress exerted on the soil particles after accounting for the pressure from the pore water. Including  $c_r$  reflects the roots' contribution to the soil's overall cohesion. Roots bind soil particles together, enhancing the soil's shear strength and making it more resistant to mechanical failure, particularly when the soil might otherwise be prone to erosion or landslides.

Cazzuffi et al., 2014, conducted direct shear tests on soil samples (63.3% Silt and 28.7% Clay) with roots (from the *Gramineae* family) and observed that the reinforcing effect provided by roots only adds an increment of cohesion. The cohesion of the root-soil system was significantly higher than that of the bare soil (i.e., about 72% for *Atriplex canescens*). The results indicate an increase in shear strength due to root reinforcement of approximately 25% (for *Atriplex canescens*) compared to the shear strength of soil without roots [14].

Tang et al., 2023, made triaxial shear tests to observe how palm fibers affect the mechanical properties of a sandy sample. The tests were carried out under consolidated drained conditions (C.D.), and the research included 16 series of remolded palm-fibres-reinforced sand samples and one series of bare sand for comparison. The study varied fiber lengths between 8 mm and 20 mm and fiber contents between 0.3% and 0.9% by mass. The results indicated that while palm fibers



contributed significantly to the *critical shear strength* (increasing by over 100%), they had a more modest effect on *peak shear strength* (increasing by about 10-20%). The analysis revealed that fiber-reinforced sand experienced different volume changes and void ratios than bare sand. Fiber content positively correlated with increased strength capacity, but it is recommended to determine the shear strength parameters on naturally grown roots, not remoulded samples [26].

Zhang et al., 2023, noticed that rainwater infiltration is crucial for rainfall-induced slope failure because the infiltrated water can significantly weaken the shear strength of unsaturated soil [16]. This conclusion is in relation to the UUsat tests conducted in our study.

#### 2.2.4. Scale Model Devices: Erosion Control Chamber and Rainfall Simulator

The study observes erosion phenomena caused by torrential rainfall in scaled models. The scale model device consists of two main components: (1) an erosion simulation chamber and (2) a rainfall simulator, both constructed from plexiglass (Figure 7).

These devices/boxes developed to simulate slope erosion were designed to meet several technical, economic, and practical requirements, including (1) constructing the model at the smallest possible scale while still accurately representing the erosion phenomenon, (2) enabling measurements that effectively capture the magnitude and dynamics of the process, (3) closely replicating the effects of torrential rainfall, (4) demonstrating the role of geosynthetic materials in erosion control, (5) assessing the utility of a topsoil layer, (6) evaluating the thickness of this layer, (7) accounting for the presence, (8) type, and (9) age of vegetation.

Six transparent plexiglass boxes, each measuring 105 cm in length, 63 cm in height, and 20 cm in thickness, were constructed for the erosion simulation chamber. The testing boxes are open-topped and designed to be in direct contact with the atmosphere while also allowing the attachment of the rainfall simulator. To ensure the boxes could support the lateral pressure developed by the soil, a plexiglass sheet thickness of 1 cm was chosen, and one metal bar was installed to maintain a constant thickness of 20 cm.

These experimental boxes were placed in an experimental plot in Chiajna, Ilfov County, Romania. From May to September 2023, they were exposed to natural climatic conditions of humidity and temperature, with the exception of the first two weeks after planting, when they were irrigated to facilitate germination and plant growth.

All experiments were recorded on video using a GoPro Hero 9, allowing observation of the dynamics of the slope erosion process and the changes in the slope profile due to the transport of displaced material from the upper to the lower part of the slope.

In the experimental boxes, artificial slopes with a 2:3 (V:H) gradient were created using very erodible soil of poorly graded medium sand. The sand was placed into the box in layers and lightly compacted by hand. Some tests were also conducted using topsoil layered onto the slopes in steps to create a bond between the two soil types. In trial tests where geosynthetic materials were used, the geomats were placed both on the slope and the horizontal surfaces. They were secured in the soil with two metal clamps, which were removed as the vegetation grew and the plants developed their root systems.

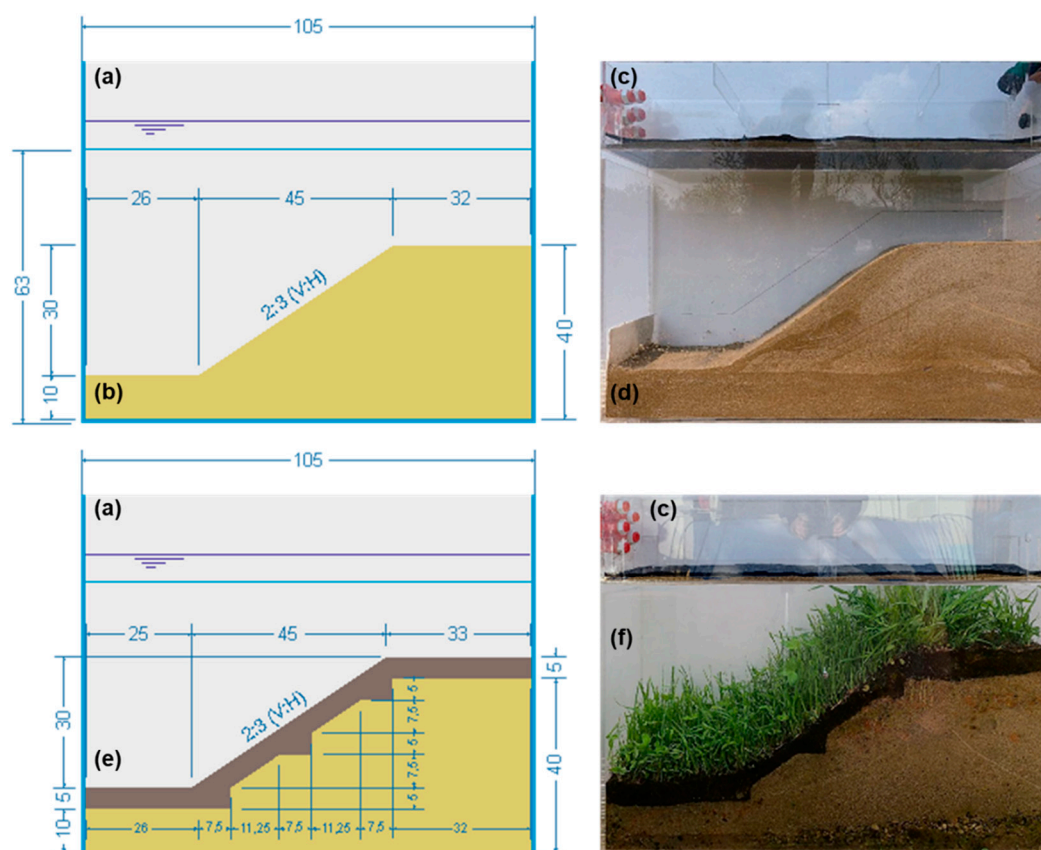


**Figure 7.** Scale model devices [27]: (a) the sketch of the rainfall simulator at the upper part, (b) the sketch of the erosion control chamber with a slope of 2:3 (V:H), (c) the image of the rainfall simulator at the upper part, (d) the image of the erosion control chamber with an artificial slope of 2:3 (V:H) realized by compacted sand (e) the sketch of the erosion control chamber with the dimensions of the artificial slope protected by a 5 cm OS layer placed in steps, and (f) the image of the erosion control chamber with an artificial slope protected by OS and mature vegetation.

The study tracks erosion through visual observation, utilizing images taken throughout the experimental process. The extent of erosion is measured by calculating the volume of soil or other material that has been eroded, moved from its original location, and then accumulated at the base of the slope. This approach allows for a detailed assessment of how much material is displaced during erosion events and where it is deposited.

A similar study conducted by He et al., 2023, revealed that sandy soil is the most problematic soil in terms of soil erosion. The research concludes that slope instability in the study area was primarily due to the soil's geotechnical properties, particularly its high permeability and low shear strength. Rainfall is critical in accelerating instability, especially under prolonged or intense conditions. The treatment measures implemented (geosynthetics and vegetation) have successfully improved slope stability [28].

The rainfall simulator is a parallelepiped box with the exact base dimensions of the erosion simulation chamber (105 x 20 cm) and a height of 20 cm. Its base is perforated with 1 mm diameter holes arranged in a square grid with one cm<sup>2</sup> spacing. It serves as a water reservoir with a perforated base, maintaining the water height at different levels to simulate varying rain intensities. The tests carried out in the experimental device consisted of simulating the effect of rain of 400 l/s, ha (144 mm/h) on a slope with a slope of 2:3 (V:H), with a height of 30 cm [27].

The research conducted by Simelane et al., 2024, investigated the effects of rainfall intensity and slope inclination on the following processes: soil water infiltration rate, soil loss due to erosion, and surface water runoff. To study these phenomena, the researchers used a rainfall simulator, which allowed them to replicate different rainfall intensities in a controlled environment on slopes with varying inclinations. This approach enabled them to evaluate the combined impact of rainfall

intensity and slope on water and soil dynamics. To reduce soil loss, the researchers emphasized the importance of proper land management, especially in areas with steep slopes and exposed to intense rainfall [29].

2.3. Climatic Conditions

The temperature and precipitation regime influences most plant processes, including photosynthesis, transpiration, respiration, germination, and flowering. If the temperature exceeds a certain threshold, heat stress occurs in plants. To analyze this, meteorological data were collected from a nearby weather station from 1 May 2023 to 1 September 2023, specifically Weather Station ID: ICHIAJNA5, Latitude/Longitude: 44.459° N, 25.978° E.

An analysis of the meteorological data (Figure 8, based on meteorological data from Weather Station ID: ICHIAJNA5) revealed that there were 78 days during the analyzed period with temperatures exceeding 30°C, meaning that 63.93% of the period when plants were developing experienced heat stress. Regarding precipitation, it was observed that over 122 days, the total rainfall was approximately 60 mm, which is insufficient for plant growth and maintenance. According to the National Meteorological Agency, 2023 was declared the hottest year since 1900 and considered one of the driest years since then.

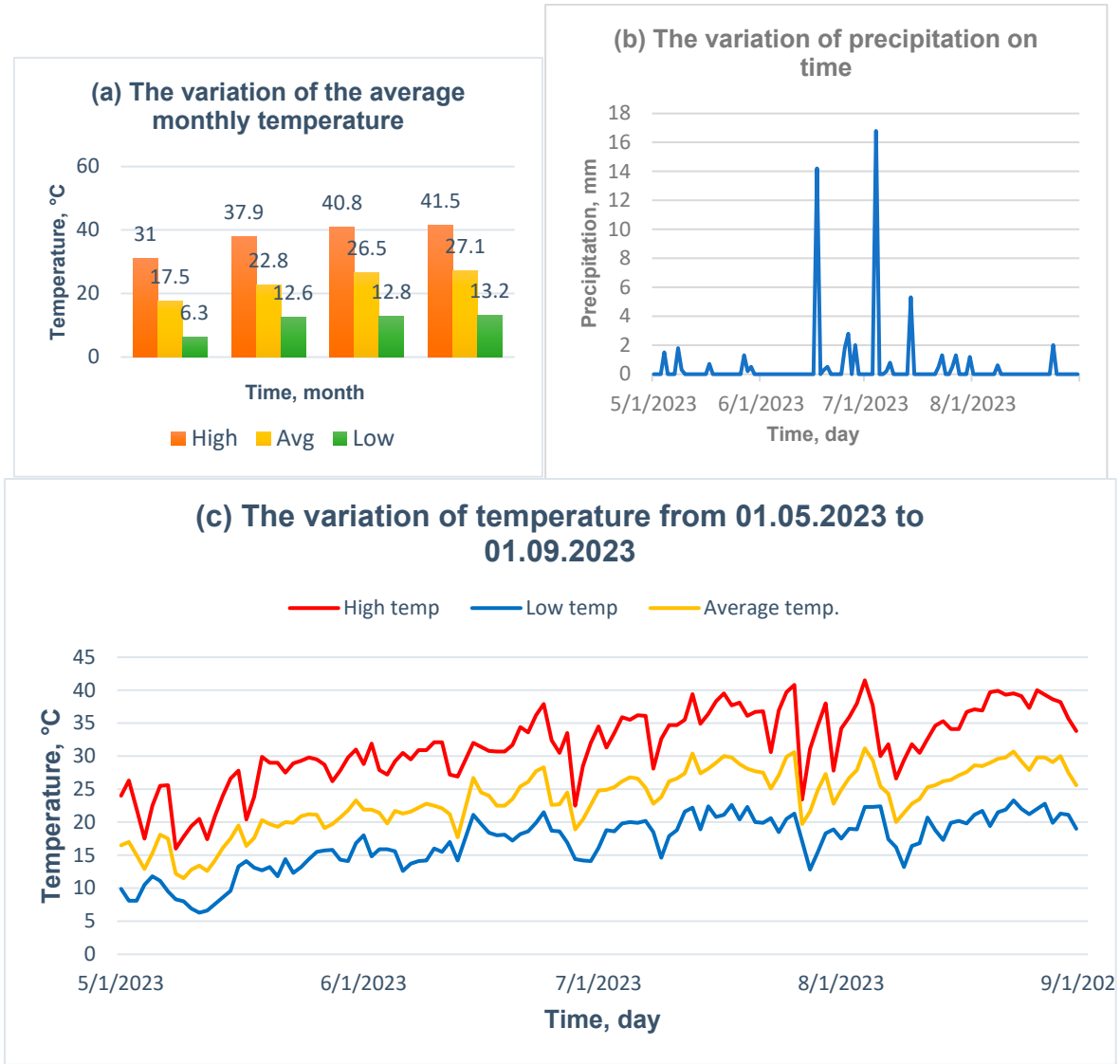


**Figure 8.** The meteorological data: (a) the variation of the highest, average, and lowest temperature recorded in May, June, July, and August 2023, (b) the variation of the precipitation recorded from 01.05.2023 to 01.09.2023, and (c) the variation of highest, average and lower daily temperature.

The research focuses on plant species native to Romanian grasslands and pastures, which are naturally adapted to the local climate conditions. However, they experience significant heat stress when temperatures rise above 30°C, with the effects becoming more severe as temperatures approach 35°C. Within this group, *Festuca arundinacea* is noted for its relative resilience, being able to endure the higher end of this temperature range (up to 35°C) better than the other species studied.

At the same time, it has been observed that changing the precipitation regime can disrupt the distribution of precipitation globally, intensifying erosion phenomena in some areas and substantially changing the water supply of the soil in other areas, all of which lead to land degradation [30].

Short-term heavy precipitation has become an important early warning indicator of rain disasters in China because these extreme rainfalls represent a primary factor in soil erosion and sediment yield [31,32]. The latest flooding disaster from Europe, in September - October 2024, was caused by short-term heavy precipitation in the catching area of rivers associated with the Danube.

### 3. Results and Discussions

#### 3.1. Optimum Organic Soil Thickness

To understand how plants develop in different thicknesses of organic and sandy soil, visual observations were made on the cylinders filled with soil and sown with herbaceous seeds presented in this paper. The tests start on 30.09.2022 by seeding Mix 1 and Mix 2 (in the simple and double number of seeds) cylindrical containers. The seeds germinated after 4 days, on 3 October 2022. Conducting this experimental program is essential for designing and correctly selecting the optimal mixtures to be sown in the erosion control chamber (transparent boxes with a length of 1.05 m, thickness of 0.20 m, and height of 0.63 m), as well as determining the optimal thickness of the OS layer for both the development of the plant root system and the improvement of shear strength parameters for the soil-root system and at the soil-sand interface.

From the sowing until 02.11.2022, the plants were watered with 50 ml of water every 3-4 days. On 02.11.2022, it was observed that the plants were showing slight water stress, and the watering rate was increased to 100 ml for the devices with 20, 15, and 10 cm of topsoil, while it remained at 50 ml for those with 5 and 0 cm of topsoil (Figure 9). The watering interval remained constant. Starting on 24.11.2022, the watering rate was increased to 150 ml for the devices with 20, 15, and 10 cm of topsoil and 100 ml for those with 5 and 0 cm of topsoil, with the remaining watering interval unchanged.

From visual observations and measurements of growth parameters from 30.09.2022 to 27.02.2023 (170 days), it was concluded that in the cylinders where a double number of seeds was sown, the results are not relevant to the research project because the density of the sprouted plants is too high, causing the plants to crowd each other and preventing proper root development. It was also observed that the plants that developed in the container with 5 cm of topsoil developed roots as strong as the plants developed in thicker layers of topsoil; this led to the conclusion that a layer of 5 cm of topsoil is optimal for the development of plants and their roots.





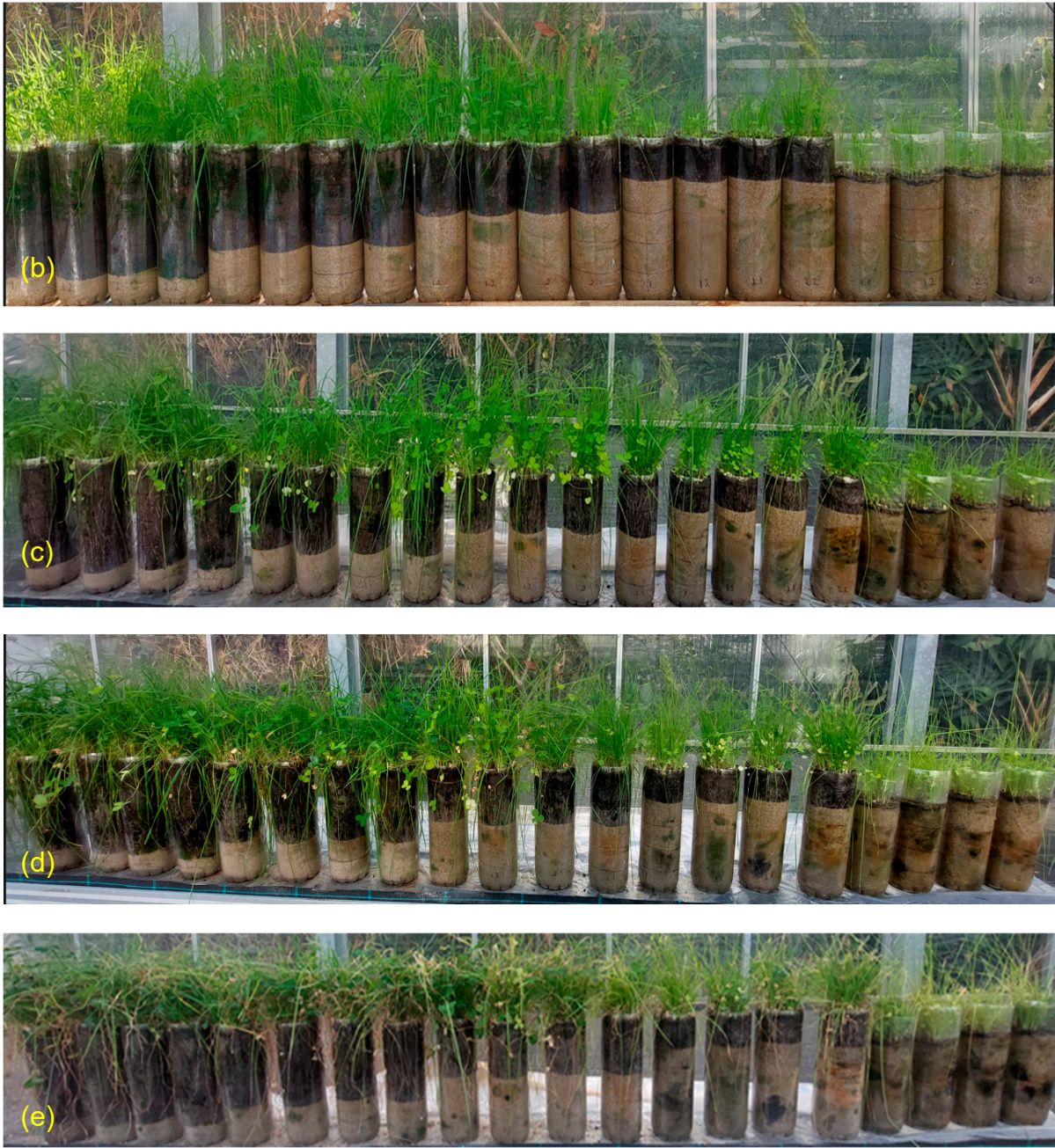
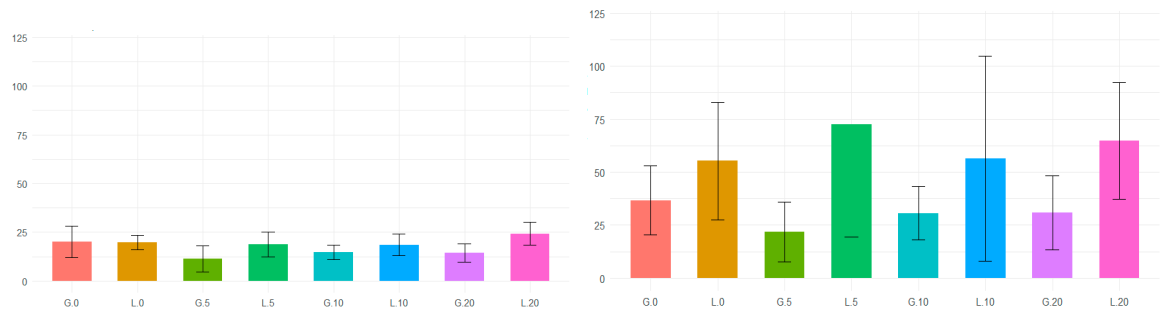


**Figure 9.** The growing plant's stages at different periods: (a) 30.09.2022 (day 0), (b) 25.10.2022 (25 days), (c) 19.11.2022 (50 days), (d) 14.12.2022 (75 days), and (e) 27.02.2023 (150 days).

3.2. Roots Characteristics

Root system development when the OS layer varies between 0 and 20 cm was analyzed. Figure 10 presents a comparison between manually measured root lengths and WinRHIZO measurements.



(a) (b)

**Figure 10.** The comparison of the influence of the OS layer thickness on root length measured (a) manually, (b) with WinRHIZO.

When we measured the absolute length of the roots, all the variants presented similar values. WinRHIZO measured length showed differences between Gramineae and Leguminous, and its methods considered all the segments, not only the direct line between the starting and ending points of the root systems. Gramineae presented lower values than Leguminous. The Gramineae plants grown in 5 and 10 cm OS layers had lower length values than those grown in 0 and 20 cm, and at Leguminous plants grown in 0 and 10 cm OS layers presented lower root developments (Figure 10).

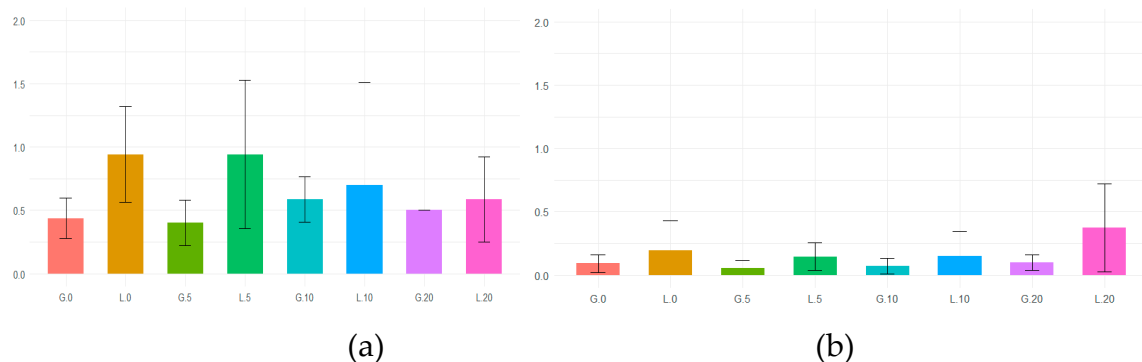


**Figure 11.** The comparison of the influence of the OS layer thickness on root volume measured (a) manually, (b) with WinRHIZO.

WinRHIZO measurements were slightly lower than the manual ones for analyzing the root volume due to the method specificity and digital precision. For Gramineae plants, those grown in 0 and 5 cm OS layers showed slightly lower values than those grown in 10 and 20 cm OS layers. For leguminous plants, those grown in 10 and 20-cm OS layers exhibited lower root development. The results differ from those of Pang et al., 2009 [24] but are similar to those of Meng-Ben and Qiang, 2009 [33], which have differences between different volume method measurements.

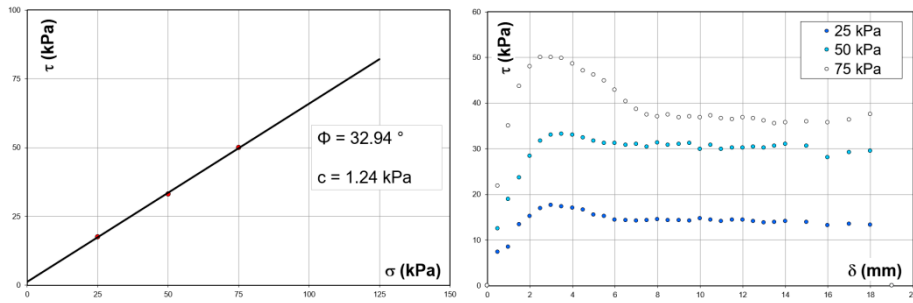
The density of roots is significant; it has been observed that soil loosening occurs after a specific root density value is reached [34]. Kaushal et al., 2020, studied the variation in root density at depths of 0–0.90 m for different bamboo species. The study found that bamboo species with higher root densities contributed significantly to soil reinforcement, water retention, and the overall enhancement of soil properties, making them highly effective for soil conservation in the Western Himalayan foothills [35].

The development of roots in soil is directly influenced by the following soil parameters: particle size, bulk density, pore size and tortuosity, suction and water content, organic matter content, and mineral composition. Simultaneously, the soil alters or improves its properties in the presence of roots based on factors such as root diameter, tensile strength, root type, root architecture, and the number and condition of roots (living or dried roots).

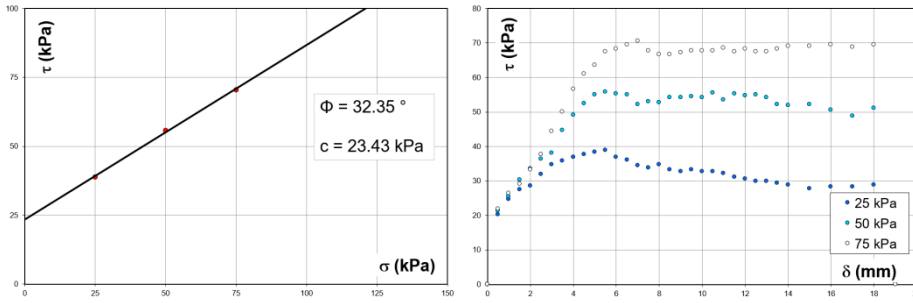
Research conducted on four types of herbaceous species by Gobinath et al., 2020, showed that roots with high tensile strength and good cellulose content act as an excellent reinforcing agent for hill slope stability [36].

### 3.3. Shear Strength Characteristics

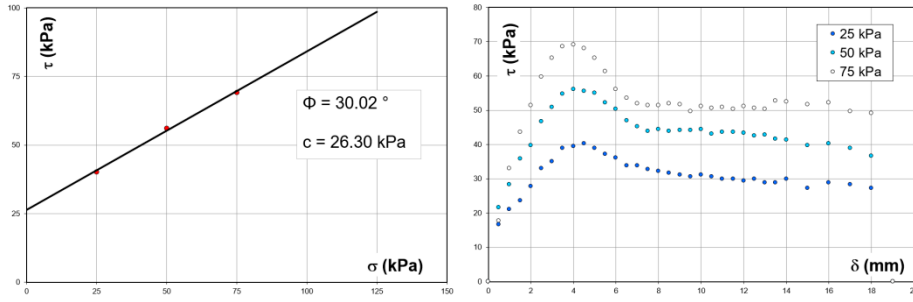
Direct shear tests were performed to assess the shear strength of various soil types. Samples were taken from different layers, as shown in Figure 12. These included bare sand (without vegetation) - BS, sand reinforced by plant roots - SR, bare OS - BO, OS with roots - OSR, and samples positioned at the boundary between the OS and sand layers, where roots were present - INT. The results allowed for comparing how roots and soil compositions influence shear resistance (Table 1).



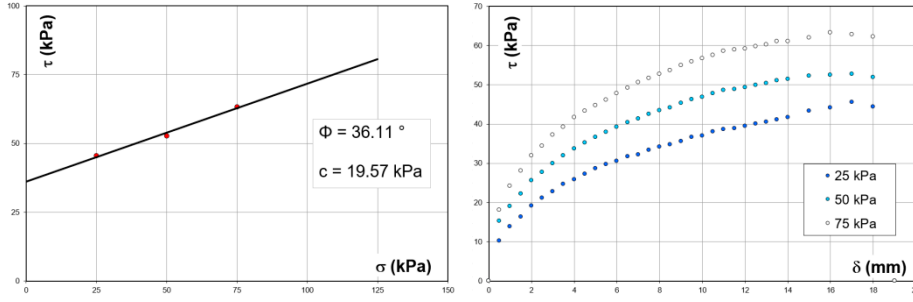
(a) bare sand (BS)



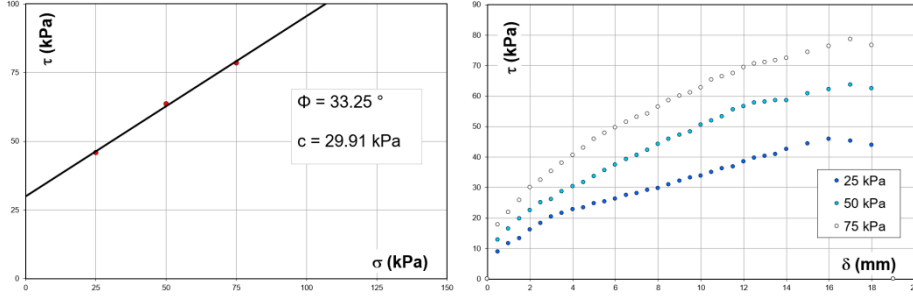
(b) sand with roots, sample collected from 0 – 5 cm depth (SR 0-5 cm)



(c) sand with roots, sample collected from 10 - 15 cm (SR 10-15cm)

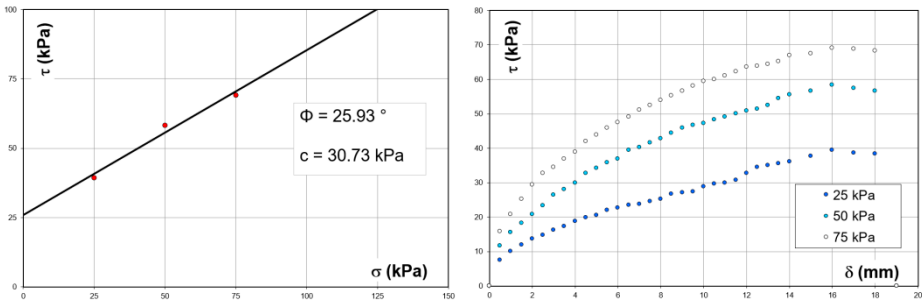


(d) bare organic soil (BO)



(e) OS with roots, a sample collected from 0 – 5 cm (OSR 0-5 cm)





(f) OS with roots, sample collected from 10 – 15 cm (OSR 10-15 cm)

**Figure 12.** Variation of shear stress vs. everyday stress (left) and shear strength vs. horizontal displacement (right) on soil/soil-roots samples [37].

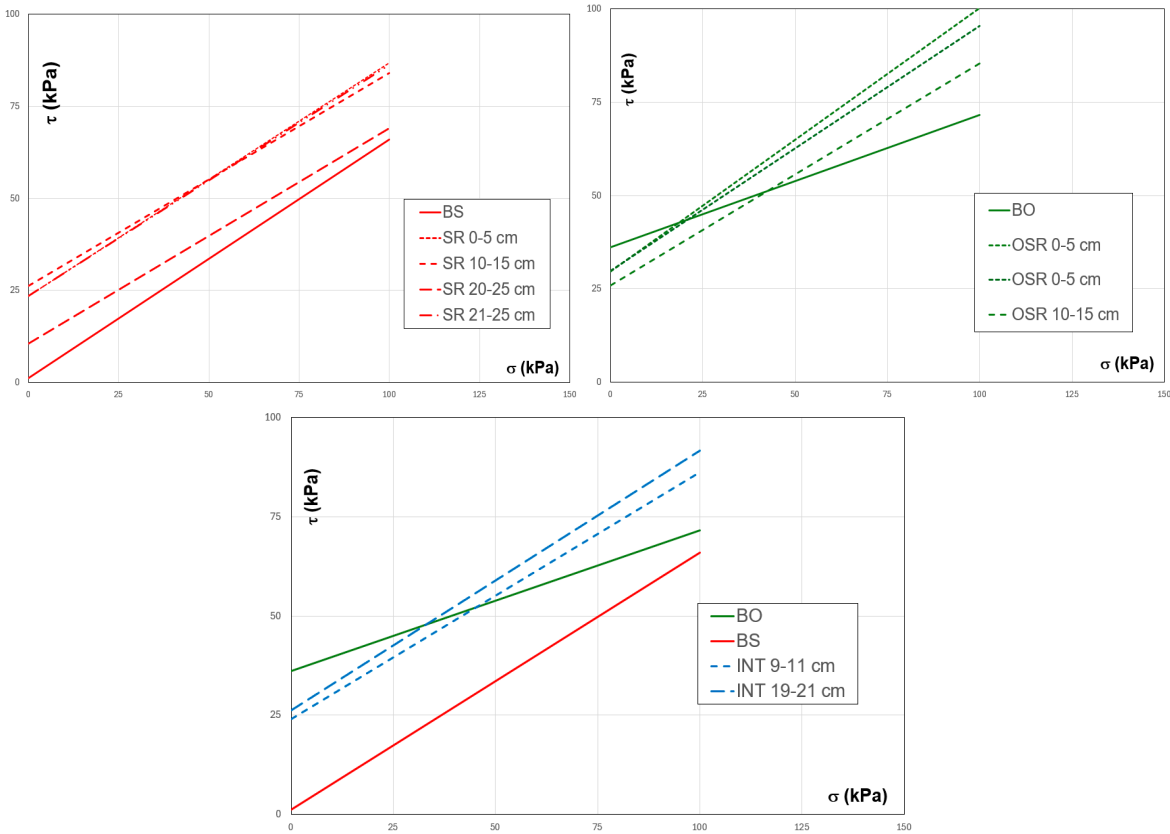


**Figure 13.** The variation of shear stress vs everyday stress on all analyzed samples: (a) sandy samples, (b) OS samples, and (c) samples collected from the interface between OS and sand [37].

The experimental results indicate that the presence of roots introduces a cohesion added by roots ( $c_r$ ) when the mechanical behavior at failure is described using Mohr-Coulomb’s law. At the same time, the shear strength angle ( $\phi$ ) remains in the same range. The summary of the results from the direct shear tests is presented in Table 1.

**Table 1.** The shear strength parameters of bare soil and soils with roots [37].

Shear strength	Sandy samples				
	BS	SR 0-5	SR 10-15	SR 20-25	SR 21-25
c (kPa)	1.24	23.43	26.3	10.65	23.52
$c_r$ (kPa)	-	22.19	25.06	9.41	22.28
$\Phi$ (°)	32.94	32.35	30.02	30.26	32.12



Shear strength	OS samples				Interface samples	
	BO	OSR 0-5	OSR 0-5	OSR 10-15	INT 10-15	INT 19-21
c (kPa)	36.11	29.72	29.91	25.93	23.98	26.2
cr (kPa)	-	-6.39	-6.2	-10.18		
$\Phi$ (°)	19.57	35.21	33.25	30.73	31.89	33.25

Based on shear strength parameters, slope stability is evaluated; the more significant the internal friction angle and the cohesion of rooted soils, the higher the slope’s stability factor. Research conducted by Li et al., 2022, showed that the shear strength parameters of rooted soils increase with the growth of root diameter. They also examined four models of root distribution in the soil, specifically with distribution angles of 0°, 30°, 60°, and 90°. The vertical root distribution model in the soil (at a 90° distribution angle) can increase cohesion by up to 150 % [23]. In our paper, the shear strength parameters were determined on natural roots, developed naturally with a distribution angle of 90°; in conclusion, all the shear strength parameters determined are at the maximum increase value.

3.4. Erosion Tests Under Rainfall Conditions

The tests conducted using the experimental model, which simulates the effect of torrential rainfall of 400 l/s,ha (144 mm/h) on a slope of 2:3 (V:H) at scale, focus on assessing the changes in the slope profile over time.

For the test performed on an unprotected sandy slope, it was observed that after a maximum of 20 minutes of rainfall, the slope experienced complete degradation, with the material being eroded and the slope reaching a gradient of approximately 1:5.5 (V) (Figure 14). The rainfall was applied for 30 minutes.

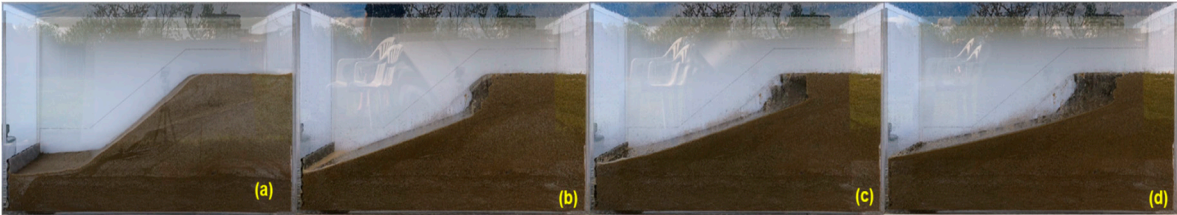


**Figure 14.** Variation of the profile for the unprotected sandy slope during a rainfall simulation at different periods [27]: (a) t = 0 minutes, (b) t = 10 minutes, (c) t = 20 minutes, and (d) t = 30 minutes.

When geosynthetic materials were used for erosion control, the onset of erosion was delayed, varying in effectiveness depending on the specific materials applied (Figures 15–17). It was observed that erosion caused by raindrops was practically eliminated, as the shape of these geosynthetic materials is specifically designed for this purpose. The displaced material was carried underneath the geosynthetic material because the soil mass was fully saturated during the rainfall simulation. The rainfall was applied for 30 minutes in the case of the slope protected by GEC 2 and 40 minutes in the case of the slope protected by GEC 1 and GEC 3. It was decided not to display the captures after 40 minutes of rainfall because the geometry of the slope remained approximately the same, the amount of eroded material was roughly the same, and it was decided that all the representations in Figure 15–17 should be on the same scale.

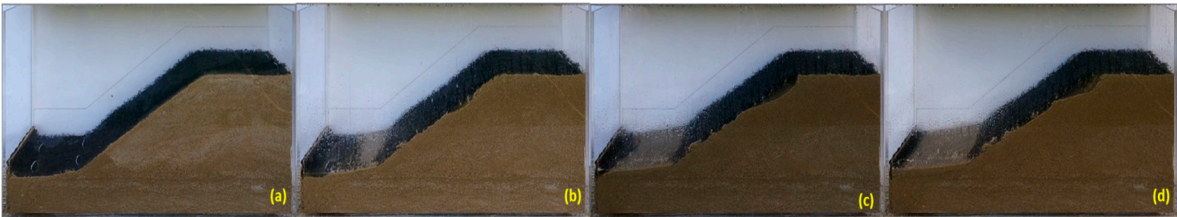


**Figure 15.** The variation in the profile of a sandy excavation unprotected and protected with GEC1 during rainfall simulation at different periods [27]: (a)  $t = 0$  minutes, (b)  $t = 10$  minutes, (c)  $t = 20$  minutes, and (d)  $t = 30$  minutes.

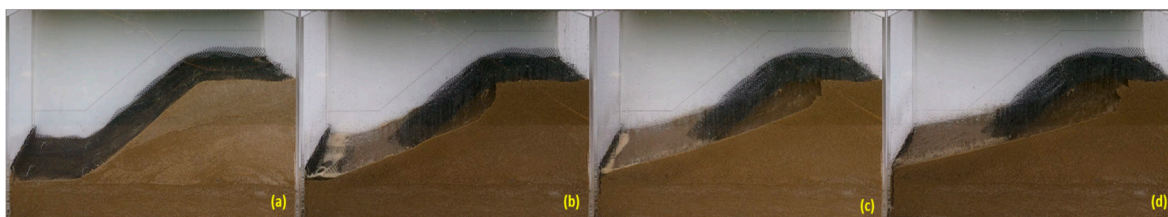


**Figure 16.** The variation in the profile of a sandy excavation unprotected and protected with GEC2 during rainfall simulation at different periods [27]: (a)  $t = 0$  minutes, (b)  $t = 10$  minutes, (c)  $t = 20$  minutes, and (d)  $t = 30$  minutes.

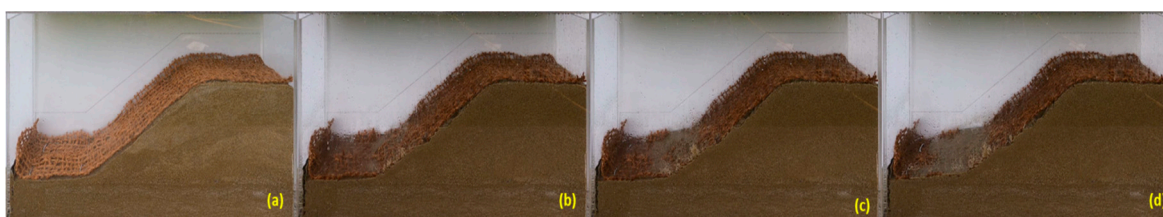


**Figure 17.** The variation in the profile of a sandy excavation unprotected and protected with GEC3 during rainfall simulation at different periods [27]: (a)  $t = 0$  minutes, (b)  $t = 10$  minutes, (c)  $t = 20$  minutes, and (d)  $t = 30$  minutes.

For the same slope, protected by a thin layer of 0.5 cm of OS and immature vegetation, no significant improvement was observed under similar rainfall conditions compared to the other tests (the slope unprotected or the slope protected by only a thin layer of OS layer). The seeds were planted on April 15, 2023, and the torrential rainfall simulation was conducted on May 14, 2023, just one month after sowing. The vegetation exhibited minimal, anemic growth, as the plants had only a very thin layer of topsoil of 0.5 cm (Figure 18). This stunted growth is correlated with the development of very thin, superficial roots, as validated in the cylindrical containers discussed in subsection 3.1.

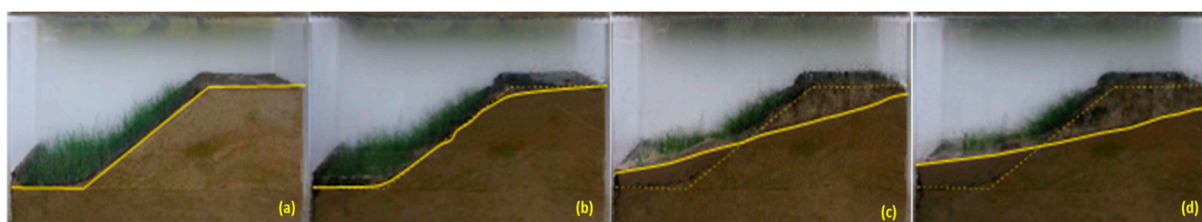


**Figure 18.** The variation in the profile of a sandy excavation protected by 0.5 cm of OS with immature vegetation during rainfall simulation at different periods [27]: (a)  $t = 0$  minutes, (b)  $t = 10$  minutes, (c)  $t = 20$  minutes, and (d)  $t = 30$  minutes.

Simulating torrential rainfall over an area where excavation had been made in sandy soil, topped with a layer of 5 cm of OS that had been seeded but where the vegetation had not yet developed, had severe effects. In the scaled model, landslides occurred, completely altering the initial profile after just 10 minutes of intense rainfall (Figure 19).





**Figure 19.** The variation in the profile of a sandy excavation protected by 5 cm of OS (with seeds) during rainfall simulation at different periods: (a)  $t = 0$  minutes, (b)  $t = 10$  minutes, and (c) after approx.—four months, during the winter.

This rapid and massive shallow landslide occurred because the topsoil, without plant roots, absorbed all the rainwater quickly, increasing its weight. Since the soil beneath the topsoil layer was not saturated, a failure plane formed below the saturated topsoil layer, causing a general instability in 10 minutes. The scale model test remained undisturbed during the winter, from January 2023 until April 2023. Because during the winter of 2023-2024, there were a few days below-freezing temperatures, the seeds germinated, sprouted, and grew. It was observed that during the landslide caused by the torrential rainfall simulation, the seedlings also slid to the base of the slope.

To observe the effect of rainfall simulation on slopes protected with 5 cm OS, vegetation, and geosynthetic materials, four erosion chambers were placed in an experimental plot located in Chiajna, Ilfov County, Romania. They were exposed to natural climatic humidity and temperature conditions from 01.05.2023 to 01.09.2023. Their evolution in two important stages can be observed in Figures 20 and 21.

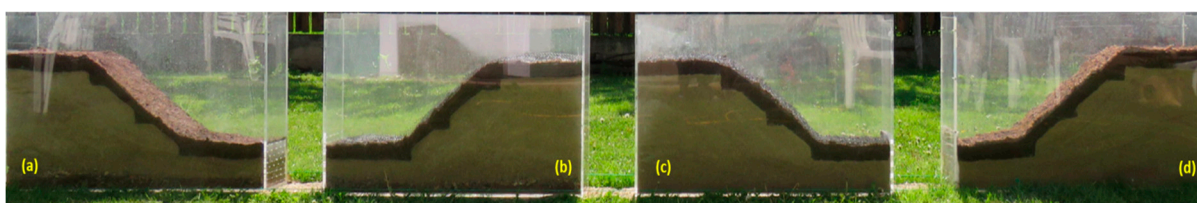


**Figure 20.** The sandy slope protected by 5 cm OS layer after seeding (01.05.2023): (a) slope protected by 5 cm OS, (b) slope protected by 5 cm OS and GEC 1, (c) slope protected by 5 cm OS and GEC 2, and (d) slope protected by 5 cm OS and GEC 3.

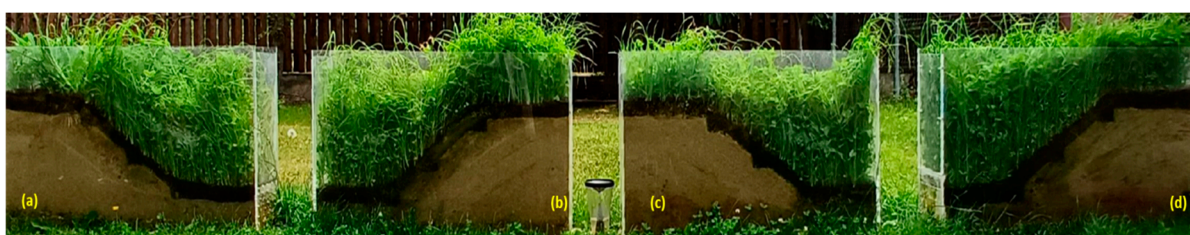


**Figure 21.** The sandy slope protected by a 5 cm OS layer and mature vegetation after 45 days of seeding (15.06.2023): (a) slope protected by 5 cm OS, (b) slope protected by 5 cm OS and GEC 1, (c) slope protected by 5 cm OS and GEC 2, and (d) slope protected by 5 cm OS and GEC 3.

The effect of mature vegetation on slope stability can be observed in Figure 22. For this test, a seed mixture was planted on May 1, 2023, consisting of *Festuca arundinacea* (25%), *Dactylis glomerata* (25%), *Phleum pratense* (20%), *Trifolium pratense* (10%), and *Trifolium repens* (20%) over a 5 cm thick layer of OS. The rainfall simulation was conducted on June 15, 2023, one and a half months after the seeds were sown. The rainfall simulation was applied at the most unfavorable time possible after trimming the plants. It was observed that mature vegetation is very effective in controlling slope erosion. After the rainfall simulation, the slope of the embankment remained the same, and no signs of erosion appeared, not even after 50 minutes.

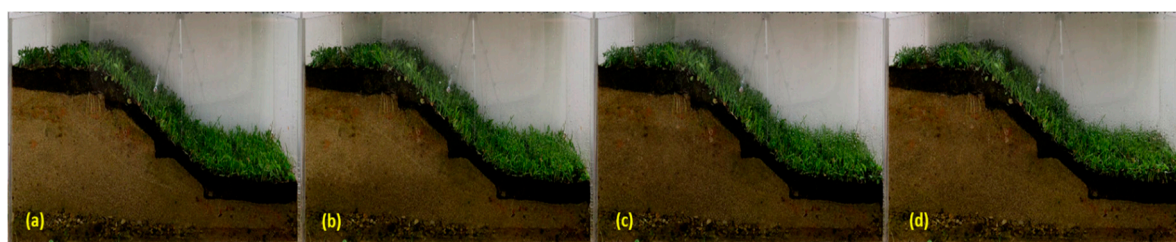


**Figure 22.** The variation in the profile of a sandy excavation protected by 5 cm of OS with trimmed mature vegetation during rainfall simulation at different periods: (a)  $t = 0$  minutes, (b)  $t = 10$  minutes, (c)  $t = 30$  minutes and (d)  $t = 50$  minutes.

This test was conducted under the most favorable conditions, when temperatures support plant growth and development and water needs are met by precipitation or irrigation. Unfortunately, the effects of climate change have also been felt by these plants, leading them to dry out by the end of the summer. To observe how plants are influenced by the increased summer temperatures and the drought caused by the lack of precipitation, the grass-covered slopes were left in natural temperature and humidity conditions until September 1, 2023. During this period, there were 78 days with temperatures exceeding  $30^{\circ}\text{C}$  and 60 mm of precipitation. These climatic conditions caused the plants to dry out, allowing for simulations of torrential rains under the most unfavorable situation: mature, dry vegetation (Figure 23).

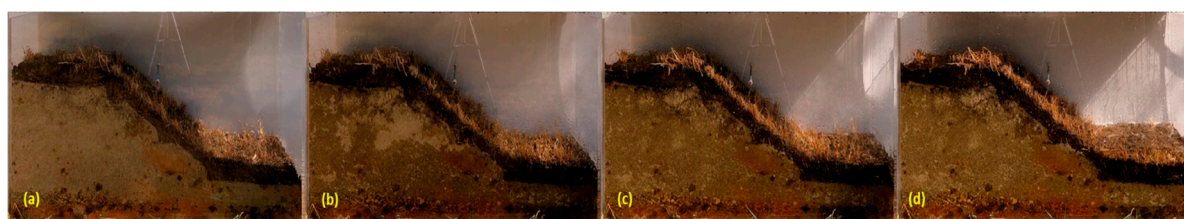


**Figure 23.** The variation in the profile of a sandy excavation protected by 5 cm of OS with dried mature vegetation during rainfall simulation at different periods: (a)  $t = 0$  minutes, (b)  $t = 10$  minutes, (c)  $t = 30$  minutes and (d)  $t = 50$  minutes.

The samples were irrigated and developed in the first two weeks after sowing, reaching maturity approximately one and a half months after sowing. After this period, they were left under the natural environmental humidity and temperature (as shown in Figures 23–27) during a summer period characterized by high temperatures and no recorded precipitation. Under these conditions, the topsoil contracted, and upon contact with the plexiglass walls of the erosion chamber, cracks of 0.3 – 0.5 mm formed. In the simulated torrential rain tests, no erosion was recorded in the entire soil mass, even with dry vegetation. Still, sand was displaced in the interface areas with the plexiglass wall.

Research on soil massive erosion will be further developed by replacing the sand with loess—a soil sensitive to moisture (a material that covers approximately 18% of Romania's territory, according to NP 125:2010 [38])—and a clayey material, predominantly used in earthworks. Another research directive focuses on modeling the scaled tests through stability calculations using limit equilibrium and finite element analysis.





**Figure 24.** The variation in the profile of a sandy excavation protected by 5 cm of OS with dried mature vegetation during rainfall simulation at different periods: (a)  $t = 0$  minutes, (b)  $t = 80$  minutes, (c)  $t = 100$  minutes and (d)  $t = 120$  minutes.

During the rainfall simulations on the slope protected by 5 cm of OS and mature dry vegetation, it was observed that the sand was displaced on the side opposite the filmed area after approximately 75 minutes, and the camera was moved. Figure 24 shows the amount of displaced material.

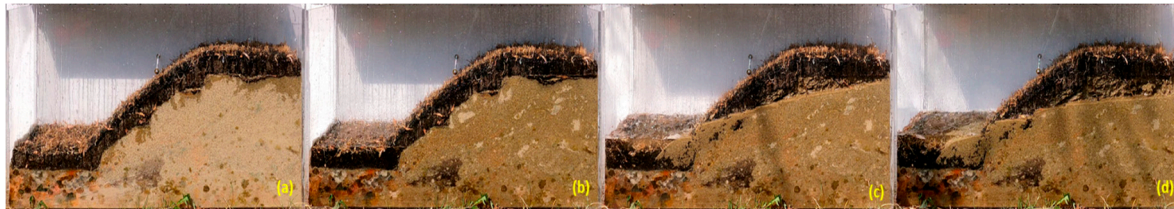


**Figure 25.** The variation in the profile of a sandy excavation protected by 5 cm of OS with dried mature vegetation and GEC 1 during rainfall simulation at different periods: (a)  $t = 0$  minutes, (b)  $t = 10$  minutes, (c)  $t = 30$  minutes and (d)  $t = 50$  minutes.

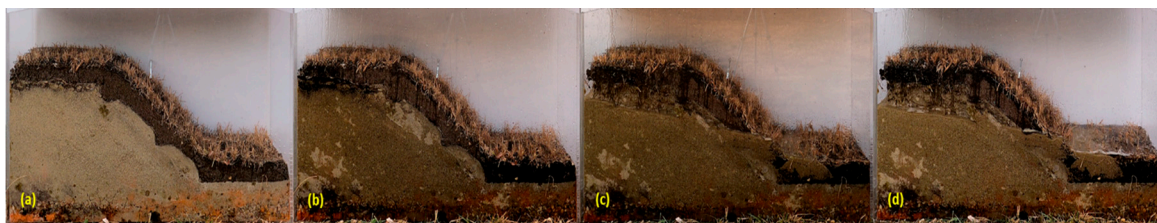


**Figure 26.** The variation in the profile of a sandy excavation protected by 5 cm of OS with dried mature vegetation and GEC 2 during rainfall simulation at different periods: (a)  $t = 0$  minutes, (b)  $t = 10$  minutes, (c)  $t = 30$  minutes and (d)  $t = 50$  minutes.

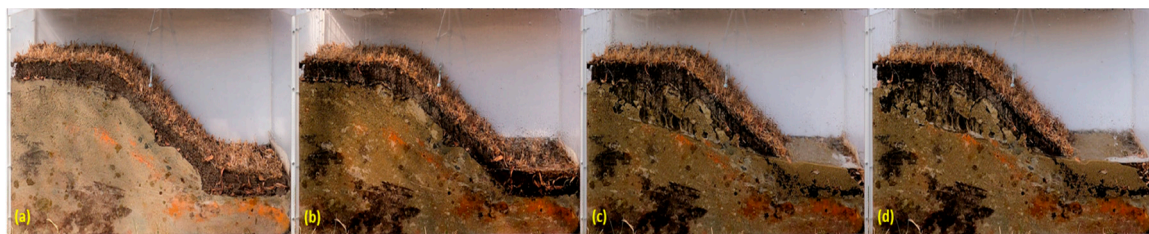


**Figure 27.** The variation in the profile of a sandy excavation protected by 5 cm of OS with dried mature vegetation and GEC 3 during rainfall simulation at different periods: (a)  $t = 0$  minutes, (b)  $t = 10$  minutes, (c)  $t = 30$  minutes and (d)  $t = 50$  minutes.

#### 4. Conclusions

Vegetation as a bio-reinforcement method is often more cost-effective and environmentally friendly than traditional engineering solutions, such as concrete. However, this bio-stabilization approach is unsuitable for applications requiring deep stabilization.

Bio-stabilization techniques contribute to the ecological restoration of slopes by supporting biodiversity and improving the aesthetic value of landscapes. The selection of appropriate species and planting techniques depends on the area's specific soil and climate conditions to ensure optimal root development and stabilization efficiency. The vegetation can be combined with other mechanical stabilization methods for hybrid approaches to slope management.

Leguminous and Gramineae plants used in slope stabilization are common in areas prone to landslides, erosion, or surface runoff. These plants are often applied to roadside slopes, riverbanks, and areas affected by deforestation or construction activities.

The roots of plants play a crucial role in stabilizing slopes by improving soil cohesion, reducing water content, and providing long-term reinforcement, making them a valuable natural solution for slope erosion control. In designing artificial slopes, an important stability analysis should be conducted for the scenario where the vegetation has dried out following a drought period. This scenario does not correspond to the scenario without vegetation, as the plant roots remain fixed in the soil and can regenerate after rainy periods.

The bio-stabilization of slopes or bio-reinforcement with living plants is a current topic that requires the involvement of specialists from Geotechnical Engineering, Agriculture, Horticulture, Environmental Engineering, and Landscaping.

**Author Contributions:** Conceptualization, T.O. and E.D.O.; methodology, T.O., E.D.O., and A.C.B.; analysis, T.O. and A.C.B.; investigation, T.O., E.D.O., and A.C.B.; resources, E.D.O.; writing—original draft preparation, T.O.; writing—review and editing, T.O., E.D.O., and A.C.B.; supervision, T.O., E.D.O. and A.C.B.; funding acquisition, T.O. All authors have read and agreed to the published version of the manuscript.

**Funding:** This research was funded by The University of Agronomic Sciences and Veterinary Medicine from Bucharest, Grant number 1068/15.06.2022, Acronym: GeoRoots.

**Institutional Review Board Statement:** Not applicable.

**Informed Consent Statement:** No humans were involved in this study.

**Data Availability Statement:** The data used in this study are available upon request from the corresponding author, as they are subject to privacy and ethical restrictions. Public access is not possible due to confidentiality agreements with the research participants.

**Conflicts of Interest:** The authors declare no conflicts of interest.

## References

1. Fatema, N.; Ansary, M. Slope stability analysis of a Jamuna River embankment. *Journal of Civil Engineering* **2014** (IEB), 42(1), pp.119-136.
2. Park, J.; Kim, I.; Kang, J.K. Root reinforcement effect on cover slopes of solid waste landfill in soil bioengineering. *Sustainability* **2021**; 13(7): 3991.
3. Hearn, G.J.; Shakya, N.M. Engineering challenges for sustainable road access in the Himalayas. *Quarterly Journal of Engineering Geology and Hydrogeology* **2017**, 50(1), pp.69-80.
4. Wu, W.; Switala, B.M.; Acharya, M.S.; Tamagnini, R.; Auer, M.; Graf, F.; Kamp, L.; Xiang, W. Effect of Vegetation on Stability of Soil Slopes: Numerical Aspect. In *Recent Advances in Modeling Landslides and Debris Flows*, 1st ed. Wu, W., Eds.; Springer Series in Geomechanics and Geoengineering, International, **2015**.
5. Masi, E.B.; Segoni, S.; Tofani, V. Root Reinforcement in Slope Stability Models: A Review. *Geosciences* **2021**, 11, 212.
6. Mao, Z.; Saint-Andre, L.; Genet, M.; Mine, F.X.; Jourdan, C.; Rey, H.; Courbaud, B.; Stokes, A. Engineering ecological protection against landslides in diverse mountain forests: choosing cohesion models. *Ecological Engineering* **2012**, 45, pp.55-69.
7. Liu, M.; Luo, Y.; Li, F.; Hu, H.; Sun, D. Experimental Research on Erosion Characteristics of Ecological Slopes under the Scouring of Non-Directional Inflow. *Sustainability* **2023**, 15(20), p.14688.
8. Ni, J.J.; Leung, A.K.; Ng, C.W.W.; Shao, W. Modelling hydro-mechanical reinforcements of plants to slope stability. *Computers and Geotechnics* **2018**, 95, pp.99-109.
9. Rimoldi, P. Design of geosynthetics for erosion control on slopes. In *Proceedings of 6th EuroGeo 6 Conference*, Ljubljana, Slovenia, 2016 Sep 25, pp. 339-360.
10. Mandal, D.; Patra, S.; Sharma, N.K.; Alam, N.M.; Jana, C.; Lal, R. Impacts of Soil Erosion on Soil Quality and Agricultural Sustainability in the North-Western Himalayan Region of India. *Sustainability* **2023**, 15(6), p.5430.
11. Singh, M.; Hartsch, K. Basics of soil erosion. In *Watershed Hydrology, Management and Modeling*, 1st ed.; Yousuf, A., Singh, M., Eds.; CRC Press: Boca Raton, Florida, USA, **2019**, pp. 1-61.
12. Kanianska, R.; Kizeková, M.; Jančová, L.; Čunderlík, J.; Dugátová, Z. Effect of Soil Erosion on Soil and Plant Properties with a Consequence on Related Ecosystem Services. *Sustainability* **2024**, 16(16), p.7037

13. Turcu, C.L.; Chiper, B.M.; Bucur, D.; Popa, N. Research on runoff and soil erosion in the Târnii Valley hydrographic basin from Tutova rolling hills, Romania, during 2019-2021. *AgroLife Scientific Journal* **2024**, *13*(1), pp.217-222.
14. Cazzuffi, D.; Cardile, G.; Giofrè, D. Geosynthetic engineering and vegetation growth in soil reinforcement applications. *Transportation Infrastructure Geotechnology* **2014**, *1*, pp.262-300.
15. Mairaing, W.; Jotisankasa, A.; Leksungnoen, N.; Hossain, M.; Ngernsaengsaruy, C.; Rangsiwanichpong, P.; Pilumwong, J.; Pramusandi, S.; Semmad, S.; Ahmmed, A.N.F. A Biomechanical Study of Potential Plants for Erosion Control and Slope Stabilization of Highland in Thailand. *Sustainability* **2024**, *16*(15), p.6374.
16. Zhang, X.; Wang, H.; Gao, Z.; Xiang, K.; Zhai, Q.; Satyanaga, A.; Chua, Y.S. Evaluation of the Performance of the Horizontal Drain in Drainage of the Infiltrated Water from Slope Soil under Rainfall Conditions. *Sustainability* **2023**, *15*(19), p.14163.
17. Cardile, G. and Pisano, M. Advances in soil reinforcement with geosynthetics: From laboratory tests to design practice. *Riv. Ital. Geotech* **2020**, *54*, pp.52-82.
18. Markiewicz, A.; Koda, E.; Kawalec, J. Geosynthetics for Filtration and Stabilisation: A Review. *Polymers* **2022**, *14*, 5492
19. Markiewicz, A.; Koda, E.; Kiraga, M.; Wrzesiński, G.; Kozanka, K.; Naliwajko, M.; Vaverková, M.D. Polymeric Products in Erosion Control Applications: A Review. *Polymers* **2024**, *16*, 2490.
20. Kim, Y.-J.; Kotwal, A.R.; Cho, B.-Y.; Wilde, J.; You, B.H. Geosynthetic Reinforced Steep Slopes: Current Technology in the United States. *Appl. Sci.* **2019**, *9*, 2008.
21. SR EN-ISO 14688-2:2018. Geotechnical investigations and tests. Identification and classification of soil. Part 2: Principles for a classification
22. Gong, C.; Ni, D.; Liu, Y.; Li, Y.; Huang, Q.; Tian, Y.; Zhang, H. Herbaceous Vegetation in Slope Stabilization: A Comparative Review of Mechanisms, Advantages, and Practical Applications. *Sustainability* **2024**, *16*(17), p.7620.
23. Li, P.; Xiao, X.; Wu, L.; Li, X.; Zhang, H.; Zhou, J. Study on the Shear Strength of Root-Soil Composite and Root Reinforcement Mechanism. *Forests* **2022**, *13*, 898.
24. Pang, W.; Crow, W.T.; Luc, J.E.; McSorley, R.; Giblin-Davis, R.M.; Kenworthy, K.E.; Kruse, J.K. Comparison of Water Displacement and WinRHIZO Software for Plant Root Parameter Assessment. *Plant Dis.* **2011** Oct; *95*(10):1308-1310
25. SR EN ISO 17892-10:2019 - Geotechnical investigations and tests. Laboratory tests of soils. Part 10: Direct shear tests
26. Tang, Y.; Wei, S.; Liu, X.; Liu, W.; Liu, T. Mechanical Analysis of Palm-Fiber-Reinforced Sand through Triaxial Tests. *Sustainability* **2023**, *15*(6), p.5461.
27. Olinic, T., Olinic, E.D. The role of geosynthetic materials and vegetation on slope erosional control: Results of scale model tests. In *E3S Web of Conferences* **2024**, Vol. 569, p. 09004.
28. He, Y.; Li, B. and Du, X. Soil slope instability mechanism and treatment measures under rainfall—A case study of a slope in Yunda Road. *Sustainability* **2023**, *15*(2), p.1287.
29. Simelane, M.P.Z.; Soundy, P.; Maboko, M.M. Effects of Rainfall Intensity and Slope on Infiltration Rate, Soil Losses, Runoff and Nitrogen Leaching from Different Nitrogen Sources with a Rainfall Simulator. *Sustainability* **2024**, *16*(11), p.4477.
30. Corches, MT. Land degradation and climate change. *Scientific Papers. Series E. Land Reclamation, Earth Observation & Surveying, Environmental Engineering* **2023**, Volume 12, pp. 69-73.
31. Chen, Z.; Xie, C.; Xiong, G.; Shen, J.; Yang, B. Using the Morgenstern–Price Method and Cloud Theory to Invert the Shear Strength Index of Tailings Dams and Reveal the Coupling Deformation and Failure Law under Extreme Rainfall. *Sustainability* **2023**, *15*(7), p.6106.
32. Li, E. Effects of Extreme Rainfall Change on Sediment Load in the Huangfuchuan Watershed, Loess Plateau, China. *Sustainability* **2024**, *16*(17), p.7457.
33. Wang, M.B.; Zhang, Q. Issues in using the WinRHIZO system to determine physical characteristics of plant fine roots. *Acta Ecologica Sinica* **2009**, *29*(2), pp.136-138.
34. Olinic, T.; Stanciu, A.M.; Butcaru, A.C.; Luchian, V. Bio-reinforcement of slopes. *Scientific Papers. Series E. Land Reclamation, Earth Observation & Surveying, Environmental Engineering* **2023**, *12*.
35. Kaushal, R.; Singh, I.; Thapliyal, S.D.; Gupta, A.K.; Mandal, D.; Tomar, J.M.S.; Kumar, A.; Alam, N.M.; Kadam, D.; Singh, D.V., and Mehta, H. Rooting behaviour and soil properties in different bamboo species of Western Himalayan Foothills, India. *Scientific reports* **2020**, *10*(1), p.4966.

36. Gobinath, R.; Ganapathy, G.P.; Salunkhe, A.A.; Raja, G.; Prasath, E.; Kavya, T. Understanding Soil Erosion Protection Capabilities of Four Different Plants on Silty Soil. In IOP Conference Series: Materials Science and Engineering, Warangal, India, December 2020, Vol. 981, No. 3, p. 032053.
37. Olinic, T.; Olinic, E.D. The effect of living plant roots on the shear strength parameters: a sustainable approach to shallow slope stability and erosion control applications. In Proceedings of the 4th International Conference on Sustainable Development in Civil, Urban and Transportation Engineering, Wroclaw, Poland, 14 October 2024, *in press*.
38. NP 125:2010 – Technical norm: Foundation on collapsible soils

**Disclaimer/Publisher's Note:** The statements, opinions and data contained in all publications are solely those of the individual author(s) and contributor(s) and not of MDPI and/or the editor(s). MDPI and/or the editor(s) disclaim responsibility for any injury to people or property resulting from any ideas, methods, instructions or products referred to in the content.